

This is a repository copy of *Site-Selective Aryl Diazonium Installation onto Protein Surfaces at Neutral pH using a Maleimide-Functionalized Triazabutadiene*.

White Rose Research Online URL for this paper:

<https://eprints.whiterose.ac.uk/201519/>

Version: Published Version

Article:

Yates, Nicholas David James, Hatton, Natasha Emily, Fascione, Martin Anthony orcid.org/0000-0002-0066-4419 et al. (1 more author) (2023) Site-Selective Aryl Diazonium Installation onto Protein Surfaces at Neutral pH using a Maleimide-Functionalized Triazabutadiene. *Chembiochem*. e202300313. ISSN 1439-7633

<https://doi.org/10.1002/cbic.202300313>

Reuse

This article is distributed under the terms of the Creative Commons Attribution (CC BY) licence. This licence allows you to distribute, remix, tweak, and build upon the work, even commercially, as long as you credit the authors for the original work. More information and the full terms of the licence here:

<https://creativecommons.org/licenses/>

Takedown

If you consider content in White Rose Research Online to be in breach of UK law, please notify us by emailing eprints@whiterose.ac.uk including the URL of the record and the reason for the withdrawal request.

Site-Selective Aryl Diazonium Installation onto Protein Surfaces at Neutral pH using a Maleimide-Functionalized Triazabutadiene

Nicholas D. J. Yates,^[a] Natasha E. Hatton,^[a] Martin A. Fascione,^{*[a]} and Alison Parkin^{*[a]}

Aryl diazonium cations are versatile bioconjugation reagents due to their reactivity towards electron-rich aryl residues and secondary amines, but historically their usage has been hampered by both their short lifespan in aqueous solution and the harsh conditions required to generate them *in situ*. Triazabutadienes address many of these issues as they are stable enough to endure multiple-step chemical syntheses and can persist for several hours in aqueous solution, yet upon UV-exposure rapidly release aryl diazonium cations under biologically-relevant conditions. This paper describes the synthesis

of a novel maleimide-functionalized triazabutadiene suitable for site-selectively installing aryl diazonium cations into proteins at neutral pH; we show reaction with this molecule and a surface-cysteine of a thiol disulfide oxidoreductase. Through photo-activation of the site-selectively installed triazabutadiene motifs, we generate aryl diazonium functionality, which we further derivatize via azo-bond formation to electron-rich aryl species, showcasing the potential utility of this strategy for the generation of photoswitches or protein-drug conjugates.

Introduction

Aryl diazonium cations will rapidly react with electron-rich aryl motifs and secondary amine motifs, via either azo-bond (Figure 1)^[1] or triazene formation^[2] under physiologically-relevant conditions. This allows aryl diazonium cation labelling of canonical residues, such as tyrosine^[1a-g,i,k,l,n] or histidine.^[1f-h] Should an even more rapid and selective labelling be required, noncanonical residues such as 5-hydroxytryptophan,^[1i] 2-amino-3-(6-hydroxy-2-naphthyl)propanoic acid,^[1j] or alkylated lysine motifs^[2] can also be installed into proteins and subsequently be labelled with aryl diazonium cations. As such, aryl diazonium cations have become popular reagents in a broad-range of applications, from the analysis of biomolecules by Ultraviolet Photodissociation Mass Spectrometry^[1h,3] to the labelling of viral capsids.^[1k,l] Additionally, both azo- and triazene bonds can be cleaved selectively; azo-bonds can be broken via treatment with sodium dithionite,^[1i,k,4] whereas triazenes cleave at low pH.^[2] As such, bioconjugations using aryl diazonium cations can be suitable for the reversible labelling of proteins. However, while aryl diazonium cations have proven themselves to be valuable reagents in the labelling of proteins, historically their utility has been somewhat restricted by their short lifespan in aqueous solution, their poor stability (complicating their synthesis and

often resulting in a limited shelf-life), and the harsh conditions required to generate them *in situ*.^[1a,c,e,f]

The triazabutadienes developed by the Jewett group^[1b-d,m,5] address many of these issues, as these species are stable enough to endure multiple-step chemical syntheses and persist for several hours in aqueous solution, yet rapidly break down upon exposure to UV-irradiation to release diazonium cations, even under biologically relevant conditions.

The majority of the triazabutadienes developed to date have been used to install bio-orthogonal functionality or fluorophores onto proteins via azo-bond formation to electron-rich aromatic residues installed within the protein.^[1b-d,i] However, a strategy has not yet been reported in which triazabutadienes are used to install aryl diazonium cations onto protein surfaces site-selectively. In this regard it is worth noting that while the highly electrophilic 4-nitrobenzenediazonium cation can be used to label tyrosine residues at physiological pH,^[1i] less electrophilic diazonium cations, such as the 4-carboxybenzenediazonium cation, only react rapidly with tyrosine residues at elevated pHs (such as at pH 9),^[1i,l] with no discernible reaction occurring within 30 min between 4-carboxybenzenediazonium cations (at a concentration of 0.5 mM) and tyrosine (at a concentration of 0.6 mM) in pH 7 phosphate buffer at rt.^[1i] As such, reaction with tyrosine residues is unlikely to occur when diazonium cations are released from triazabutadienes via treatment with UV-irradiation at 0 °C at near-neutral pH. This presents a tantalizing opportunity with respect to the site-selective installation of diazonium cation functionality onto the surface of proteins for subsequent bioconjugation to other targets.

Herein we report the synthesis of a novel maleimide-functionalized triazabutadiene (X), and showcase its usage in the site-selective labelling of a cysteine mutant of DsbA (a bacterial thiol disulfide oxidoreductase)^[6] (Figure 1, left), fol-

[a] Dr. N. D. J. Yates, Dr. N. E. Hatton, Dr. M. A. Fascione, Dr. A. Parkin
 Department of Chemistry, University of York
 Heslington, York, YO10 5DD (UK)
 E-mail: martin.fascione@york.ac.uk
 alison.parkin@york.ac.uk

Supporting information for this article is available on the WWW under <https://doi.org/10.1002/cbic.202300313>

© 2023 The Authors. ChemBioChem published by Wiley-VCH GmbH. This is an open access article under the terms of the Creative Commons Attribution License, which permits use, distribution and reproduction in any medium, provided the original work is properly cited.

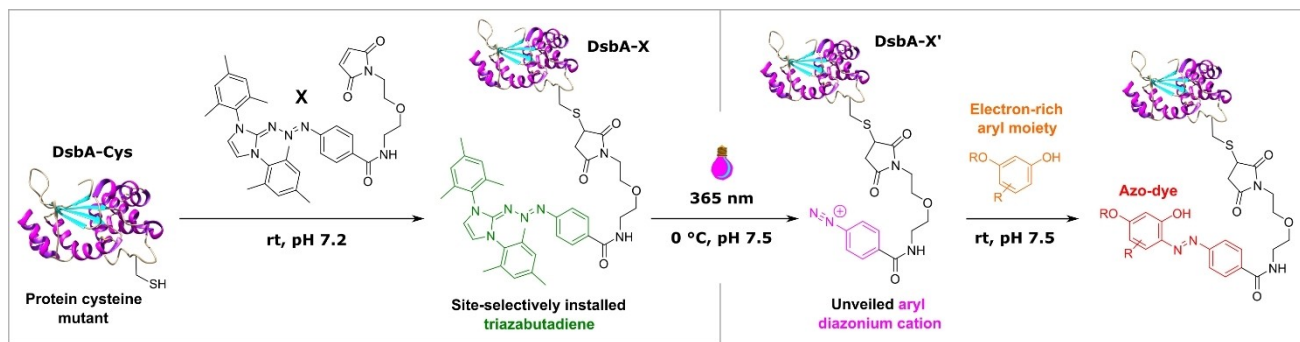


Figure 1. A strategy for the site-selective installation and derivatization of aryl diazonium cation functionality into proteins via the reaction of maleimide-functionalized triazabutadiene **X** with surface-exposed cysteine residues (left), followed by UV photoactivation and derivatization via azo dye formation (right). Images were generated using PDB ID: 4K6X.

lowed by the UV-unveiling of aryl diazonium cations^[5b] which can be utilized in subsequent bio-conjugations to electron-rich pi systems (Figure 1, right).

Results and Discussion

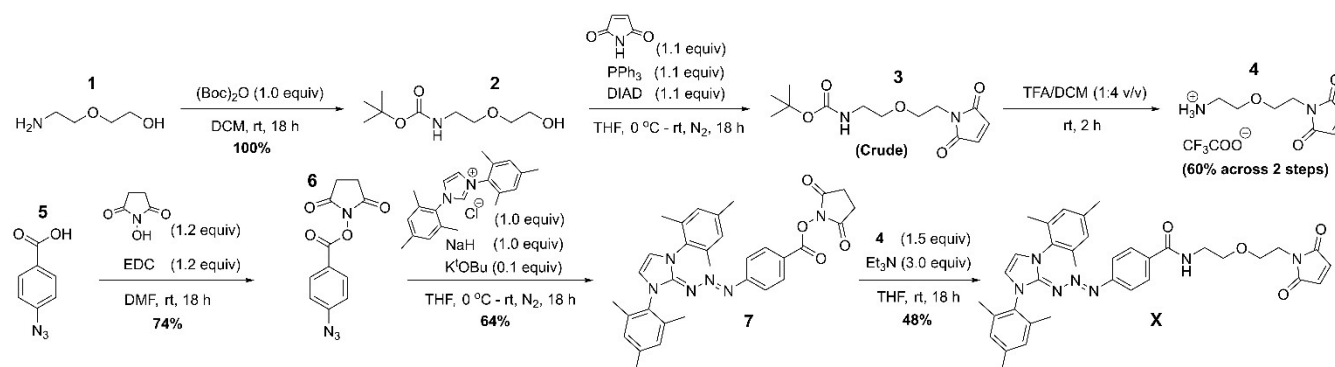
Cysteine has long been an important amino acid in the preparation of protein bioconjugates; its nucleophilic nature enables facile conjugation to electrophiles while its relatively low natural abundance on protein surfaces allows either naturally occurring residues, or those installed using site-selective mutagenesis, to be targeted site-selectively/specifically.^[7] Many mature bioconjugation chemistries have been developed for covalent crosslinking to cysteine residues, and of these chemistries, maleimide ligation is arguably the most popular, being both rapid and selective for cysteine thiols between pH 6.5 and 7.5.^[8] We therefore opted to employ a maleimide ligation for site-selective installation of a triazabutadiene motif onto proteins, via the creation of maleimide-functionalized triazabutadiene **X** (Scheme 1).

The synthesis of **X** involves the reaction of maleimide-functionalized linker **4** with NHS-ester functionalized triazabutadiene **7** (Scheme 1). While previous literature syntheses of **7** are

4-steps long,^[5b] we report a 2-step synthesis of **7** from the commercially available compound 4-azidobenzonic acid (**5**). Maleimide-functionalized linker **4** was synthesized in three steps from commercially available 2-(2-aminoethoxy)ethanol **1**, via Boc-protection of the amine functionality to yield **2**, followed by a Mitsunobu reaction and Boc-removal.

We demonstrated that the maleimide functionality in triazabutadiene **X** was able to label a cysteine residue via reaction with a mutant DsbA protein. Wild-type DsbA contains both a structural disulfide and an active-site disulfide within the protein core, but no surface cysteine. Thus, by using our so-called “DsbA-Cys” variant, which contains a single surface-cysteine in addition to the four naturally occurring core residues (Figure 3A), we had the opportunity to probe the cysteine-selectivity of reaction between a protein and **X**.

Maleimide ligation was achieved by incubating DsbA-Cys with 10 equivs of **X** in pH 7.2 buffer at rt for 30 min. Thorough removal of excess **X** was achieved through use of His-SpinTrapTM columns and buffer-exchange. UV-vis analysis of the protein showed that post-reaction with **X**, a broad absorption band centered at 390 nm is observable, which is attributable to triazabutadiene motifs (Figure 2A).^[5d] The increased absorbance at 280 nm is also attributed to the multiple aromatic motifs in **X** (Figure 2A). Conjugates of **X** and DsbA-Cys (henceforth referred



Scheme 1. The synthesis of maleimide-functionalized triazabutadiene **X**.

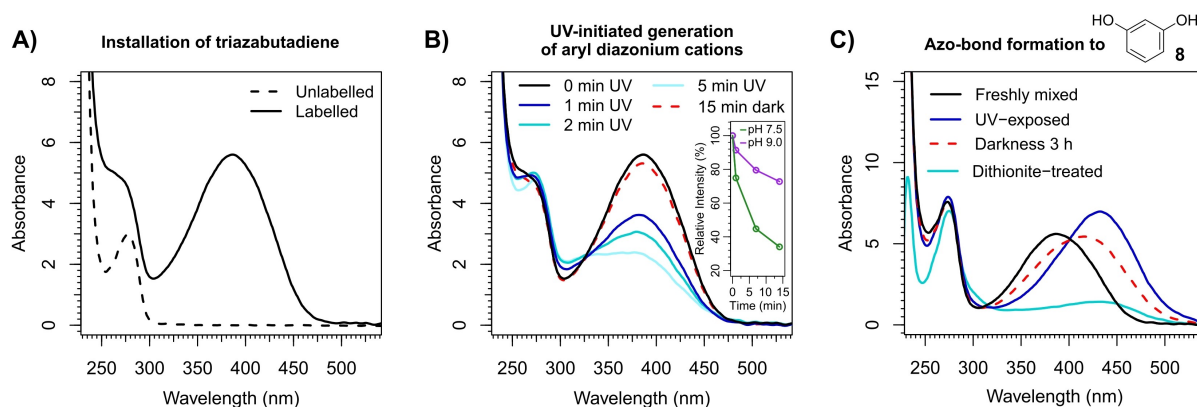


Figure 2. (A) UV-vis spectra of $\sim 100 \mu\text{M}$ samples of **Dsba-Cys** (“Unlabelled”) and **Dsba-X** (“Labelled”). (B) The monitoring of the degradation of the triazabutadiene motif installed on **Dsba-X** in response to UV irradiation at 0°C in pH 7.5 (20 mM sodium phosphate buffer), see Experimental Section. (Inset) A comparison between the pH 7.5 experiment and an analogous dataset from a pH 9.0 experiment, see Figure S3 for raw data. (C) UV-vis analysis of mixtures formed from combining **Dsba-X** ($\sim 100 \mu\text{M}$) with an excess of resorcinol, **8**, in the presence and absence of different levels of UV-irradiation and dithionite-treatment (see Main text).

to as **Dsba-X**) and their corresponding aryl diazonium-cation functionalized derivatives (henceforth referred to as **Dsba-X'**) were also detected by MS (Figure 3B). Trypsin digestion experiments indicated that under our reaction conditions compound **X** reacted with the surface-exposed mutant cysteine residue of **Dsba-Cys** in preference to the structural and active-site disulfide cysteine residues (see SI, Figures S10–12).

Next, we demonstrated the ability to rapidly unveil aryl diazonium cation motifs on the surface of **Dsba-X** via exposure to UV-irradiation from a 365 nm source (see Experimental Section). UV-vis analysis shows a rapid decrease in the intensity of the triazabutadiene absorption band upon exposure to UV irradiation (Figure 2B) at pH 7.5, which is consistent with the degradation of the triazabutadiene into aryl diazonium cations.^[5d] The rate at which this degradation occurs is notably slower at pH 9, which is consistent with the triazabutadiene behaving as a photobasic functional group (see Figure 2B inset and Figure S3).^[5d]

The importance of pH in tuning the rate of triazabutadiene-to-diazonium conversion is further illustrated by our ESI-LC/MS

results. In the analysis of a **Dsba-X** sample exposed to UV irradiation, **Dsba-X'** becomes the sole protein species identifiable after deconvolution (Figure 3, panels B and C). However, even in samples incubated in darkness there is a prominent peak attributable to the diazonium **Dsba-X'** species (Figure 3B), presumably because formic acid in the mobile phase causes rapid conversion of the acid-labile triazabutadiene into a diazonium cation, even in the absence of UV irradiation.

Having established the utility of molecule **X** for installing diazonium cations onto proteins in a site-selective manner, we then demonstrated that the aryl diazonium cations unveiled on the surface of **Dsba-X'** could be subsequently coupled to resorcinol **8** via the formation of an azo-bond. **Dsba-X** was mixed with an excess of **8** and a UV-vis spectrum was recorded of this mixture prior to its exposure to the 365 nm UV-light source (Figure 2C, “Freshly mixed”). An aliquot of this reaction mixture was then exposed to the 365 nm UV-light source for 5 min at 0°C , and was subsequently incubated in the dark for 1 h. A UV-vis spectrum of this aliquot was then recorded, and the presence of an azo-bond in the reaction product could

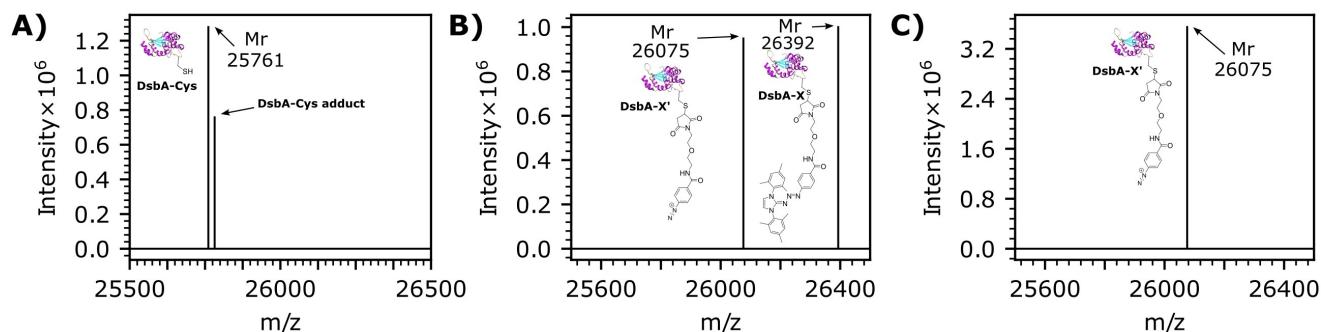


Figure 3. Deconvoluted mass spectra from positive ion mode ESI-LC/MS analysis of **Dsba** samples. (A) A sample of **Dsba-Cys**. (B) A sample of **Dsba-X** incubated in darkness. (C) A sample of **Dsba-X** that has been exposed to UV irradiation for 5 min at 0°C . Calculated Mr values for protein species are as follows; **Dsba-Cys**: 25763 Da, **Dsba-X**: 26397 Da, **Dsba-X'**: 26078 Da. Note that the presence of intra-protein disulfide bonds within the protein would reduce the mass by as much as 4 Da from what is calculated based on amino acid sequence alone.

be confirmed by the appearance of a new band centered between 430–450 nm (Figure 2C, “UV-exposed”).^[11] A second aliquot was identically treated, but was incubated with sodium dithionite prior to recording its UV-vis spectrum. The depletion of the UV-absorbance features in the region 320–600 nm for this aliquot (Figure 2C, “Dithionite-treated”) further demonstrates that the reaction between **DsbA-X** and **8** generates azo-bonds, as it is well established that incubation with sodium dithionite destroys azo-dye chromophores via reduction to anilines.^[11,k,4]

MS evidence further supports UV-activated azo-bond formation in mixtures of **8** and **DsbA-X** (see SI, Figure S7). Due to the well-documented ionization-induced fragmentation of azo-dyes during mass spectrometry,^[9] we found it prudent to do this experiment under two different ionization conditions. Comprehensive analysis of this data is presented in Figure S9. Summation of the putative azo-dye derived fragmentation peaks and the intact azo-dye peaks would suggest the conversion of diazonium functionalized DsbA to azo-bonded conjugate to be at least 74% (see SI for full discussion).

In the UV-free control experiment, in which an aliquot of the reaction mixture of **DsbA-X** and **8** was incubated in the dark (Figure 2C, “Darkness 3 h”), azo-bond formation was observed to a far lesser degree. In fact, as shown in Figure S4, we can accurately model the dark-only dataset via a linear combination of 54% “UV-exposed” and 46% “freshly mixed”, providing a quantitative measure of the substantial role that just 5 min of UV-exposure played in accelerating the rate of formation of the diazonium cation intermediate.

Finally, to demonstrate the utility of molecule **X** in enabling the labelling of a protein with a biologically relevant motif, we synthesized the novel α -mannose presenting resorcinol-functionalized probe **9** (Figure 4A), as described in the SI. Following reaction of **X** with **DsbA-Cys**, UV-promoted reaction of the **DsbA-X** product with **9** yielded a neoglycoprotein,^[10] as validated in subsequent SDS-PAGE and lectin-blot analyses (Figure 4B). While protein bands are clearly visible in all lanes of the SDS-PAGE gel, the only sample responsive to mannose-specific concanavalin A lectin blotting is in lane 6 (Figure 4B, white arrows), wherein **DsbA-X** was exposed to UV irradiation in the presence of **9**. Notably, no lectin blot band was observed in the absence of UV-activation. This is consistent with the previous results shown in Figure 2 and Figure 3, which illustrate that after **X** has been installed onto a protein using the maleimide motif, rapid conversion of the triazabutadiene motif into a diazonium cation at neutral pH requires UV exposure.

Evidence that **X** can be used to enable ligation between a protein and an electron-rich aryl motif via azo-bond formation was again provided via several different measurements. Firstly, UV-vis analysis of the product neoglycoprotein showed the depletion of the triazabutadiene absorption band to have occurred concomitantly with the growth of an azo-bond feature (Figure S5). Secondly, the treatment of the product neoglycoprotein with sodium dithionite rendered lane 7 irresponsive to lectin blotting (Figure 4B), which is consistent with the reductive cleavage of the azo-bond linkage between the DsbA protein and **9**.^[11,k,4]

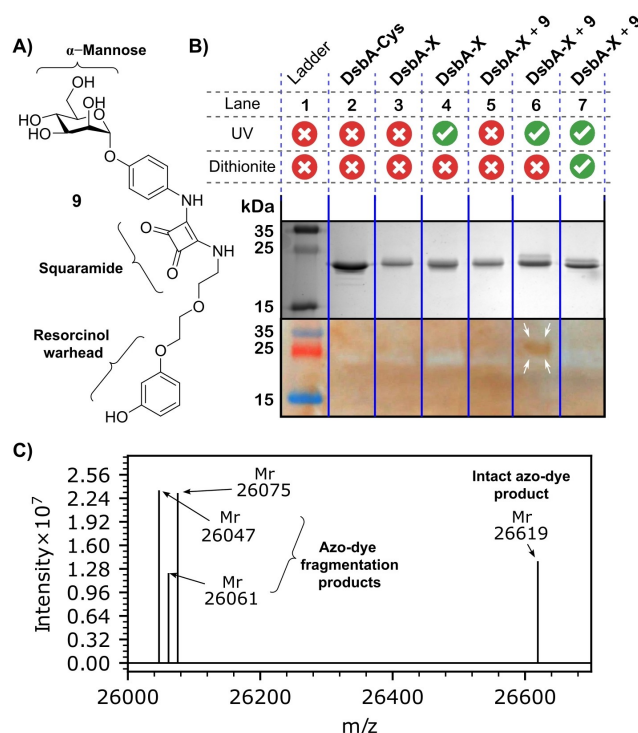


Figure 4. A) The structure of novel α -mannose presenting resorcinol-functionalized probe **9**. B) 15% polyacrylamide SDS-PAGE gel and lectin blot analyses of **DsbA** samples subjected to various treatments involving probes **X** and **9**. The SDS-PAGE gel (top) was stained with Coomassie dye. The lectin blot (bottom) was obtained using a Concanavalin A lectin-HRP conjugate and a 3,3'-diaminobenzidine color development solution. C) Deconvoluted mass spectra from positive ion mode ESI-LC/MS analysis of the neoglycoprotein yielded by the UV-promoted reaction of the **DsbA-X** product with **9**. The calculated Mr value for the DsbA-Azo dye derived from **9** is 26624Da, and the additional peaks are likely attributable to fragmentation of the azo-dye (Figure S9). Note that the presence of intra-protein disulfide bonds within the protein would reduce the mass by as much as 4 Da from what is calculated based on amino acid sequence alone.

The neoglycoprotein was also characterized via ESI-LC/MS (Figure 4C, Figure S8). Again, due to the characteristic ionization-induced azo-bond fragmentation,^[9] a summation methodology was used to evaluate the yield of the azo-bond forming bioconjugation step. Such analysis suggests this conversion to be at least 68% (see SI for full discussion). Trypsin digestion further verified that site-selective azo-bond formation had taken place during the reaction of **DsbA-X** with **9** at the site of the surface exposed mutant cysteine residue (see SI).

Conclusions

To conclude, we have reported the synthesis of a maleimide-functionalized triazabutadiene **X** and have demonstrated that it can be conjugated to protein cysteine residues. While many reports of protein bioconjugation utilize triazabutadienes as sources of functionalized diazonium cations that can bioconjugate to tyrosine residues, we report an inverted approach, demonstrating that **X** can be conjugated to proteins site-selectively via its maleimide motif while remaining intact, but

can subsequently be rapidly photocleaved to reveal diazonium cations on the surface of the protein. These diazonium cations can subsequently be ligated to probes bearing electron-rich aryl systems via azo-bond formation, and this azo-bond is readily cleaved by incubation with the highly water-soluble reducing agent sodium dithionite. Notably, there was no evidence of undesirable side-reactions between the unveiled aryl diazonium functionalities and aromatic amino acid residues.

Proceeding via our stepwise methodology ((i) protein + X, (ii) triazabutadiene-protein + UV light + resorcinol → azo-dye functionalized protein) enables facile purification of the intermediate triazabutadiene-protein conjugates, and this could enable a library of azo-dye functionalized proteins to be assembled rapidly from often-cheap commercially available aromatic compounds, without the need to isolate and purify a library of pre-synthesized azo-dye probes. We anticipate that this method may facilitate the rapid development of cleavable protein-drug conjugates. However, we note that our molecule X could also be utilized in one-pot conjugation methodologies, or even in more conventional i) UV light + resorcinol → azo-dye, ii) protein + azo-dye → azo-dye functionalized protein methods.

Experimental Section

Chemical synthesis

Complete syntheses and characterizations of X and 9 are described in the SI.

Protein Production

Full details of the production of DsbA-Cys are provided in the SI.

Preparation of DsbA-X

To 450 μL of a 110 μM solution of DsbA-Cys in pH 7.2 buffer (20 mM sodium phosphate) was added tris(2-carboxyethyl)phosphine (TCEP) (100 equivs, 45 μL of a pre-neutralized 100 mM stock of TCEP hydrochloride). The resultant solution was incubated at rt in darkness for 20 min. After this time, the protein was exchanged into fresh pH 7.2 buffer (20 mM sodium phosphate + 500 μM TCEP) using a PD MiniTrap™ G-25 desalting column - 1 mL of a 37 μM solution of DsbA-Cys was recovered. 10 equivs of X were then delivered to the protein solution, via the addition of 100 μL of a 3.7 mM solution of X in DMSO. The resultant solution was incubated in darkness for 30 min. His-SpinTrap™ columns (cytiva) were then used to remove excess probe, as detailed in the SI. Upon elution of the protein, imidazole was removed via exchanging the protein sample into pH 7.5 buffer (20 mM sodium phosphate) using a PD MiniTrap™ G-25 desalting column, yielding 1 mL of a 34 μM solution of DsbA-X which was concentrated to 100 μM using a 10 kDa MWCO centrifugal concentrator. The resultant protein was aliquoted into 90 μL aliquots and flash-frozen for later use.

UV-irradiation: source and exposure method

UV irradiation of samples was performed using a commercially available UV nail curing product - the nailstar® 36-Watt Professional

UV Nail Lamp (Model: NS-01-UK&EU). This product is fitted with 4 replaceable 9 W U-shaped tube bulbs that emit at 365 nm and has a mirrored interior.

Samples were introduced to quartz cuvettes which were stood in a shallow dish of icy water inside the nailstar®. UV-irradiation was then supplied for the specified duration.

UV-vis analysis

Tracking the UV-initiated conversion of DsbA-X to DsbA-X'

Data shown in Figure 2B was generated via an experiment which commenced with 20 μL of a 100 μM sample of DsbA-X in pH 7.5 buffer (20 mM sodium phosphate). 16 μL of the sample was placed in a quartz cuvette stood in a shallow dish of icy water in the nailstar® instrument, while the other 4 μL was stored in a sealed vial in darkness at rt. An initial 2 μL aliquot was withdrawn from the cuvette sample and analysed using the nanodrop function of a DeNovix instrument (see SI), to generate data labelled as "0 min UV". The remainder of this bulk protein sample was then subjected to 1 min of UV-irradiation at 0 °C, with UV-vis analysis of a further 2 μL aliquot generating the "1 min UV" data. Subsequent stop-start of the UV-irradiation and analysis of aliquots generated the "2 min UV" and "5 min UV" datasets of Figure 2B. The UV-vis spectrum of the sample of DsbA-X that was incubated in darkness was recorded after storage for 15 min ("15 min dark").

Validating azo-bond formation between DsbA-X and 8 via UV-vis

To 20 μL of a 100 μM sample of DsbA-X in pH 7.5 buffer (20 mM sodium phosphate) was added 1.8 μL of a 10 mM stock of 8 in DMSO (9 equivs). The resultant mixture was then split into two samples. One sample was set aside and kept in darkness at rt for 3 h, and after this time a UV-vis spectrum was recorded. For the other half of the bulk sample, an initial UV-vis spectrum was taken of a 2 μL aliquot, then the remaining volume was subjected to 5 min of 365 nm UV-irradiation at 0 °C and was subsequently incubated at rt for 1 h. After this time a second UV-vis spectrum was recorded of a 2 μL aliquot. The UV-exposed sample was then treated with sodium dithionite (final concentration 50 mM) for 1 h at rt, after which time a final UV-vis spectrum was recorded. All the data is shown in Figure 2C.

Validating azo-bond formation between DsbA-X and 9 via UV-vis

To 300 μL of a ~5 μM sample of DsbA-X in pH 7.5 buffer (20 mM sodium phosphate) was added 30 μL of a 20 mM stock of 9 in DMSO (~400 equivs). The resultant mixture was then split into two 150 μL samples. One sample was set aside and kept in darkness at rt for 1 h. An initial UV-vis spectrum was recorded of the other sample, then it was subjected to 2 min of 365 nm UV-irradiation at 0 °C, and was subsequently incubated at rt for 1 h. After this time both samples were exchanged into 150 μL of fresh pH 7.5 buffer (20 mM sodium phosphate) using a PD SpinTrap™ G-25 column and flash-frozen for later use. These samples were analysed using UV-vis (see SI, Figure S5).

Protein Mass Spectrometry

High Performance Liquid Chromatography-Electrospray Ionization Mass Spectrometry (ESI-LCMS) of protein samples was performed

using a Dionex UltiMate® 3000 Ci Rapid Separation LC system equipped with an UltiMate® 3000 photodiode array detector probing at 250–400 nm, coupled to a HCT ultra ETD II (Bruker Daltonics) ion trap spectrometer, using Chromeleon® 6.80 SR12 software (ThermoScientific), esquireControl version 6.2, Build 62.24 software (Bruker Daltonics), and Bruker compass HyStar 3.2-SR2, HyStar version 3.2, Build 44 software (Bruker Daltonics) at CoEMS. Protein samples were analysed without the use of a column at RT. Mass spectrometry data analysis was performed using ESI Compass 1.3 DataAnalysis, version 4.4 software (Bruker Daltonics). All mass spectrometry was conducted in positive ion mode unless stated otherwise. The esquireControl “Compound Stability” setting was set at “100%” unless stated otherwise.

Mass Spectrometry of DsbA-X

45 µL of a 100 µM sample of DsbA-X in pH 7.5 buffer (20 mM sodium phosphate) was exchanged into 150 µL of HPLC-grade water using a PD SpinTrap™ G-25 column. 5 µL of this protein sample was added to 45 µL of a solution of 1:1 water:acetonitrile (v/v)+1% (v/v) formic acid. The sample was then immediately analysed by mass spectrometry.

Mass Spectrometry of DsbA-X'

45 µL of a 100 µM sample of DsbA-X in pH 7.5 buffer (20 mM sodium phosphate) was exposed to 365 nm UV-irradiation for 5 min at 0 °C. The sample was then immediately exchanged into 150 µL of HPLC-grade water using a PD SpinTrap™ G-25 column. 5 µL of this protein sample was then added to 45 µL of a solution of 1:1 water:acetonitrile (v/v)+1% (v/v) formic acid and the sample was immediately analysed by mass spectrometry.

Validating azo-bond formation between DsbA-X and 8/9 via mass spectrometry

To 90 µL of a 100 µM sample of DsbA-X in pH 7.5 buffer (20 mM sodium phosphate) was added 10 µL of a 20 mM stock of **8** or **9** in DMSO (20 equivs). The sample was subjected to 10 minutes of 365 nm UV-irradiation at rt, and was subsequently incubated at rt for 2.5 h. After this time the samples were exchanged into 1 mL of HPLC-grade water using PD MiniTrap™ G-25 desalting columns. The samples were then concentrated to a volume of 100 µL. Prior to analysis via mass spectrometry, 10 µL aliquots of these protein samples were added to 40 µL of 1:1 water:acetonitrile (v/v)+1% (v/v) formic acid solution. The “compound stability” setting in the esquireControl software was set as either 100% or 60% during data collection (see SI).

SDS-PAGE and lectin blot analysis

Probing azo-bond formation between DsbA-X and **9**

To 300 µL of a 100 µM sample of DsbA-X in pH 7.5 buffer (20 mM sodium phosphate) was added 30 µL of a 20 mM stock of **9** in DMSO (20 equivs). The resultant mixture was then split into two 150 µL samples. One sample was set aside and kept in darkness at rt for 1 h. The other sample was subjected to 10 min of 365 nm UV-irradiation at rt and was subsequently incubated at rt for 1 h. After this time the samples were exchanged into 150 µL of fresh pH 7.5 buffer (20 mM sodium phosphate) using a PD SpinTrap™ G-25 column and flash-frozen for later use. SDS-PAGE gel, lectin blot, and trypsin digestion analyses were performed using these samples.

Prior to running on the gel, one UV-exposed sample was treated with sodium dithionite (final concentration 50 mM) for 1 h at rt.

SDS-PAGE gels samples were mixed with a 5 × concentrated non-reducing buffer (10% SDS, 20% glycerol, 200 mM Tris-HCl pH 6.8, 0.05% bromophenol blue) and were not boiled prior to running on the SDS-PAGE gel. Lectin blotting was performed using a Concanavalin A lectin-HRP conjugate and was visualised using a 3,3'-diaminobenzidine colour development solution. Full gel running conditions and blot preparation is detailed in the SI. Typically, ~3 µg of purified protein was loaded into each gel lane when conducting SDS-PAGE and lectin blot analysis.

Supporting Information

Additional references cited within the supporting information.^[5b,9,11]

Acknowledgements

Funding for NDJY and AP was provided by EP/X027724/1 – ERC Consolidator Guarantee Grant – Enzyme e-map – Modernising Electrochemical Enzymology To Map Electron Transfer. MAF and NEH thank UK Research and Innovation (UKRI, EP/X023680/1) for project grant funding. We thank Dr Adam A. Dowle, Dr Tony Larson, and Dr Chris J. Taylor from the University of York Bioscience Technology Facility, Metabolomics and Proteomics lab, Department of Biology; Dr Ed Bergstrom and The York Centre of Excellence in Mass Spectrometry. The York Centre of Excellence in Mass Spectrometry was created thanks to a major capital investment through Science City York, supported by Yorkshire Forward with funds from the Northern Way Initiative, and subsequent support from the Engineering and Physical Sciences Research Council (EP/K039660/1; EP/M028127/1).

Conflict of Interests

The authors declare no conflict of interest.

Data Availability Statement

The data that support the findings of this study are openly available at <https://doi.org/10.15124/a273a520-5aa9-4f65-8e00-d052a1178a01>.

Keywords: protein modifications · azo compounds · photolysis · protecting groups

- [1] a) N. Griebenow, S. Greven, M. Lobell, A. M. Dilmaç, S. Bräse, *RSC Adv.* **2015**, *5*, 103506–103511; b) M. Shadmehr, G. J. Davis, B. T. Mehari, S. M. Jensen, J. C. Jewett, *ChemBioChem.* **2018**, *19*, 2550–2552; c) A. N. Wijetunge, G. J. Davis, M. Shadmehr, J. A. Townsend, M. T. Marty, J. C. Jewett, *Bioconjugate Chem.* **2021**, *32*, 254–258; d) B. M. Cornali, F. W. Kimani, J. C. Jewett, *Org. Lett.* **2016**, *18*, 4948–4950; e) J. Gavriluk, H. Ban, M. Nagano, W. Hakamata, C. F. Barbas, *Bioconjugate Chem.* **2012**,

- 23, 2321–2328; f) D. Alvarez Dorta, D. Deniaud, M. Mevel, S. G. Gouin, *Chem. Eur. J.* **2020**, *26*, 14257–14269; g) S. Leier, S. Richter, R. Bergmann, M. Wuest, F. Wuest, *ACS Omega*. **2019**, *4*, 22101–22107; h) J. R. Aponte, L. Vasicek, J. Swaminathan, H. Xu, M. C. Koag, S. Lee, J. S. Brodbelt, *Anal. Chem.* **2014**, *86*, 6237–6244; i) P. S. Addy, S. B. Erickson, J. S. Italia, A. Chatterjee, *J. Am. Chem. Soc.* **2017**, *139*, 11670–11673; j) S. Chen, M. L. Tsao, *Bioconjugate Chem.* **2013**, *24*, 1645–1649; k) J. M. Hooker, E. W. Kovacs, M. B. Francis, *J. Am. Chem. Soc.* **2004**, *126*, 3718–3719; l) T. L. Schlick, Z. Ding, E. W. Kovacs, M. B. Francis, *J. Am. Chem. Soc.* **2005**, *127*, 3718–3723; m) N. R. Cornejo, B. Amofah, A. Lipinski, P. R. Langlais, I. Ghosh, J. C. Jewett, *Biochem.* **2022**, *61*, 656–664; n) P. A. Szijj, K. A. Kostadinova, R. J. Spears, V. Chudasama, *Org. Biomol. Chem.* **2020**, *18*, 9018–9028.
- [2] O. Nwajiobi, S. Mahesh, X. Streety, M. Raj, *Angew. Chem. Int. Ed. Engl.* **2021**, *60*, 7344–7352.
- [3] J. S. Brodbelt, L. J. Morrison, I. Santos, *Chem. Rev.* **2020**, *120*, 3328–3380.
- [4] H. Mutlu, C. M. Geiselhart, C. Barner-Kowollik, *Mater. Horiz.* **2018**, *5*, 162–183.
- [5] a) L. E. Guzman, F. W. Kimani, J. C. Jewett, *ChemBioChem*. **2016**, *17*, 2220–2222; b) S. M. Jensen, F. W. Kimani, J. C. Jewett, *ChemBioChem*. **2016**, *17*, 2216–2219; c) F. W. Kimani, J. C. Jewett, *Angew. Chem. Int. Ed.* **2015**, *54*, 4051–4054; d) J. He, F. W. Kimani, J. C. Jewett, *J. Am. Chem. Soc.* **2015**, *137*, 9764–9767; e) J. He, F. Kimani, J. Jewett, *Synlett*. **2017**, *28*, 1767–1770.
- [6] K. M. Bocian-Ostrzycka, M. J. Grzeszczuk, A. M. Banas, E. K. Jagusztyn-Krynicka, *Appl. Microbiol. Biotechnol.* **2017**, *101*, 3977–3989.
- [7] a) J. M. Chalker, G. J. L. Bernardes, Y. A. Lin, B. G. Davis, *Chem. Asian J.* **2009**, *4*, 630–640; b) Y. Kim, S. O. Ho, N. R. Gassman, Y. Korlann, E. V. Landorf, F. R. Collart, S. Weiss, *Bioconjugate Chem.* **2008**, *19*, 786–791.
- [8] D. P. Nair, M. Podgórski, S. Chatani, T. Gong, W. Xi, C. R. Fenoli, C. N. Bowman, *Chem. Mater.* **2014**, *26*, 724–744.
- [9] a) D. S. Bhagat, P. B. Chavan, W. B. Gurnule, S. K. Shejul, I. V. Suryawan-shi, *Mater. Today: Proc.* **2020**, *29*, 1223–1228; b) M. Cai, M. Jin, L. K. Weavers, *Ultrason. Sonochem.* **2011**, *18*, 1068–1076; c) X. Liu, J. L. Yang, J. H. Li, X. L. Li, J. Li, X. Y. Lu, J. Z. Shen, Y. W. Wang, Z. H. Zhang, *Food Addit. Contam. Part A Chem. Anal. Control Expo. Risk Assess.* **2011**, *28*, 1315–1323; d) M. A. Zayed, G. G. Mohamed, M. A. Fahmey, *J. Therm. Anal. Calorim.* **2011**, *107*, 763–776; e) M. Holčapek, K. Volná, D. Vaněrková, *Dyes Pigment.* **2007**, *75*, 156–165.
- [10] R. McBerney, J. P. Dolan, E. E. Cawood, M. E. Webb, W. B. Turnbull, *JACS Au* **2022**, *2*, 2038–2047.
- [11] a) T. Klein, G. Kickelbick, *Dalton Trans.* **2020**, *49*, 9820–9834; b) J. L. Gustafson, T. K. Neklesa, C. S. Cox, A. G. Roth, D. L. Buckley, H. S. Tae, T. B. Sundberg, D. B. Stagg, J. Hines, D. P. McDonnell, J. D. Norris, C. M. Crews, *Angew. Chem. Int. Ed.* **2015**, *54*, 9659–9662; c) T. Bunchuay, A. Docker, A. J. Martinez-Martinez, P. D. Beer, *Angew. Chem. Int. Ed.* **2019**, *58*, 13823–13827; d) A. Cervi, Y. Vo, C. L. L. Chai, M. G. Banwell, P. Lan, A. C. Willis, *J. Org. Chem.* **2021**, *86*, 178–198; e) M. U. Ahmad, S. M. Ali, A. Ahmad, S. Sheikh, P. Chen, I. Ahmad, *Chem. Phys. Lipids.* **2015**, *186*, 30–38; f) J. Zhang, B. Zhang, J. Zhou, J. Li, C. Shi, T. Huang, Z. Wang, J. Tang, *J. Carbohydr. Chem.* **2011**, *30*, 165–177; g) F. Beiroth, T. Koudelka, T. Overath, S. D. Knight, A. Tholey, T. K. Lindhorst, *Beilstein J. Org. Chem.* **2018**, *14*, 1890–1900.

Manuscript received: April 20, 2023
Revised manuscript received: June 1, 2023
Accepted manuscript online: June 13, 2023
Version of record online: July 18, 2023